

1                   **The influence of earthquake gates on surface rupture length**

2                   **A.M. Rodriguez Padilla** <sup>1,2\*</sup>, **M.E. Oskin**<sup>1</sup>, **E.E. Brodsky**<sup>3</sup>, **K. Dascher-Cousineau**<sup>4</sup>, **V.**  
3                   **Herrera**<sup>5</sup>, **S. White**<sup>6,7</sup>

4                   <sup>1</sup> Department of Earth and Planetary Sciences, University of California, Davis

5                   <sup>2</sup> Now at Division of Geological and Planetary Sciences, California Institute of Technology

6                   <sup>3</sup> Department of Earth and Planetary Sciences, University of California, Santa Cruz

7                   <sup>4</sup> Department of Earth and Planetary Sciences, University of California, Berkeley

8                   <sup>5</sup> Department of Earth and Environmental Sciences, San Diego State University

9                   <sup>6</sup> Geology Department, Pasadena City College

10                  <sup>7</sup> Now at Department of Earth, Planetary, and Space Sciences, University of California, Los  
11 Angeles

12  
13                  \*Corresponding author: Alba M. Rodriguez Padilla ([alba@caltech.edu](mailto:alba@caltech.edu),  
14 [amrodriguezpadilla@gmail.com](mailto:amrodriguezpadilla@gmail.com))

15                  **Key Points:**

- 16                  ● We map step-overs, bends, gaps, splays, and strands from 31 strike-slip surface ruptures  
17                  at 1:50,000 scale and investigate their potential as earthquake gates.
- 18                  ● Most step-overs wider than 1.2 km and bends with angles  $>30^\circ$  consistently halt  
19                  propagating ruptures, suggesting surficial complexity extends to depth.
- 20                  ● Our findings support that earthquake gates limit the size of large events.

21

22

23

24

25

26 **Abstract**

27 Propagating earthquakes must overcome geometrical complexity on fault networks to grow into  
28 large, surface rupturing events. We map step-overs, bends, gaps, splays, and strands of length  
29 scales ~100-500 meters from the surface ruptures of 31 strike-slip earthquakes, recording whether  
30 ruptures propagated past the feature. We find that step-overs and bends can arrest rupture and  
31 develop a statistical model for passing probability as a function of geometry for each group. Step-  
32 overs wider than 1.2 km, single bends larger than  $32^\circ$ , and double bends larger than  $38^\circ$  are  
33 breached by rupture half of the time. ~20% of the ruptures terminate on straight segments. We  
34 examine how the distribution of earthquake gates influences surface rupture length, inferring an  
35 exponential relationship between rupture length and event probability for a given fault. Our  
36 findings support that earthquake gates limit the size of large events and help discriminate between  
37 different proposed models of rupture propagation.

38

39

40 **Plain Language Summary**

41 Zones of geometrical complexity along faults can behave as barriers or earthquake gates that  
42 sometimes halt propagating earthquakes. We map five types of geometrical complexities from  
43 historical surface rupture maps and regional fault maps: step-overs, bends, gaps, splays, and  
44 strands at 1:50,000 scale, corresponding to features >100-500 m in length. This is a finer scale  
45 than previous studies, which focused on kilometer-scale zones of geometrical complexity. We  
46 classify each mapped zone of geometrical complexity as breached (earthquake propagated past) or  
47 unbreached (earthquake halted) and measure the width of step-overs and strands, the length of  
48 gaps, and the angle of splays and bends. Based on these measurements, we model the probability  
49 that each feature will be breached given its geometry. Step-overs wider than 1.2 km, single bends  
50 larger than  $32^\circ$ , and double bends larger than  $38^\circ$  are breached by rupture half of the time. ~20%  
51 of the ruptures terminate on straight segments. Using our probabilities, we show that the presence  
52 and geometry of earthquake gates in the 100-500 m length scale plays a first-order control on the  
53 low likelihood of large surface rupturing earthquakes.

54

55

56

**57 Introduction**

58 Earthquake surface ruptures are composed of fault segments bound by zones of geometrical  
59 complexity (e.g., Wesnousky, 2006; Manighetti et al., 2007; Klinger, 2010; Perrin et al., 2016;  
60 Hamling et al., 2017). These zones of geometrical complexity can act as earthquake gates where  
61 the probability of rupture propagation is conditional on prior earthquake history, rupture dynamics,  
62 material properties, and the stress conditions on neighboring fault segments. For earthquakes on  
63 vertically dipping strike-slip faults, where the thickness of the seismogenic zone limits down-dip  
64 rupture propagation, geometrical complexities have been proposed to exert an important control  
65 on rupture length, and thus magnitude (e.g., Wesnousky, 2006).

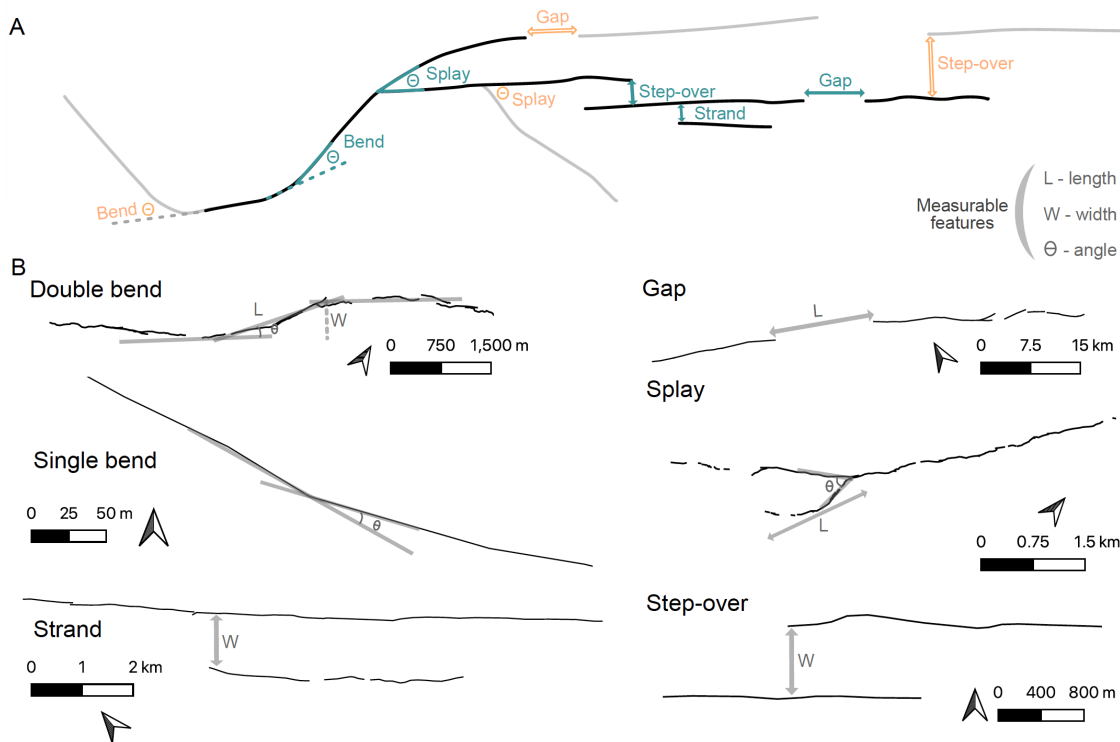
66 Historical earthquake rupture maps provide tests for geometrical controls on rupture  
67 propagation that serve as validation for rupture simulator forecasts and dynamic rupture models  
68 (e.g., Lettis et al., 2002; Wesnousky, 2006, 2008; Biasi and Wesnousky, 2016, 2017, 2021). Most  
69 previous studies relied on simplified rupture maps, limiting the minimum size of earthquake gates  
70 considered to kilometer-scale. This scale is practical for hazard applications, as it is comparable to  
71 the resolution of complexity on regional fault maps and is commensurable with model  
72 discretization in rupture simulators (Biasi and Wesnousky, 2021; Milner et al., 2022).

73 Though limited in potential for prospective hazard assessment, observations suggest that  
74 finer scale geometrical complexity can also exhibit earthquake gate behavior. For example, the  
75 2014 Napa earthquake terminated in a 750-meter-wide step-over, too small to be included in most  
76 previous studies. With new surface rupture maps from recent events, concurrent with ongoing  
77 efforts to standardize past rupture maps (e.g., Sarmiento et al., 2021; Nurminen et al., 2022) and  
78 improve regional fault maps, it is now possible to consider whether finer scale geometrical  
79 complexity can act as an earthquake gate and how the distribution of this complexity influences  
80 the probability of rupture propagation and final event size.

81 In this study, we map geometrical complexities at 1:50,000 scale, which corresponds with  
82 features >100-500 meters in length scale, from 31 strike-slip surface rupture maps in the unified  
83 Fault Displacement Hazard Initiative (FDHI) database (Sarmiento et al., 2021) and their  
84 corresponding regional fault maps (see supplementary methods). We consider five types of  
85 geometrical complexity: step-overs, bends, splays, gaps, and strands (Figure 1). Step-overs are  
86 spaces between neighboring, parallel, overlapping faults. Bends are locations where the fault  
87 changes strike. Bends may come in pairs (double bends) where the fault returns to its original

88 orientation. Step-overs and double bends may be classified as a restraining (net contraction) or  
 89 releasing (net extension), but single bends cannot be classified as such without knowledge of  
 90 rupture propagation direction. Gaps are spaces between coplanar faults, distinct from step-overs,  
 91 where faults are not coplanar. Splays are locations where the fault branches. We also consider fault  
 92 strands that are parallel to subparallel of the continuous, main rupture that are activated without  
 93 the rupture reaching the terminus of the main fault.

94 From our maps, we estimate the passing probabilities of the different features as a function  
 95 of their geometry, characterizing their potential as earthquake gates. Using these probability  
 96 distributions, we analyze the joint probability of the observed breached gates and straight segments  
 97 for each event and characterize the relationship of these probabilities to the observed surface  
 98 rupture length.



99  
 100 **Figure 1.** Geometrical complexity mapped in this study. (a) Simplified cartoon showing the  
 101 features characterized. The black lines denote the surface rupture whereas the light gray lines  
 102 represent the regional faults that did not rupture during the event. The widths, lengths, and angles  
 103 measured are shown in teal for the breached features and in orange for the unbreached features.  
 104 (b) Examples of breached features from the FDHI rupture map database (Sarmiento et al., 2021).

105

**106 What geometrical complexities act as earthquake gates?**

107 We classify each mapped feature as breached or unbreached, depending on whether the  
108 rupture propagated past the feature. To consider the size and geometry distribution of the  
109 earthquake gates we map, we estimate empirical cumulative distribution functions (ECDFs) for  
110 each population (Figure 2), separated into breached and unbreached groups, and restraining and  
111 releasing categories when possible. We infer that features with statistically distinct breached and  
112 unbreached populations are likely to act as earthquake gates, where passing probability is  
113 conditional in part on geometry. We use the two-sample Kolmogorov-Smirnoff (KS) test to assess  
114 whether different subset groups of an earthquake gate are statistically different. We use the p-value  
115 derived from the test, which is the probability of rejecting the null hypothesis that samples in the  
116 two subset groups were drawn from the same distribution. The convention here for statistical  
117 significance is  $p < 0.05$ .

118 We mapped a total of 71 step-overs, where 26 are releasing and 45 are restraining. The  
119 widest breached step-over is  $\sim 1.8$  km wide and restraining. The breached and unbreached step-  
120 over populations are distinct, though the restraining and releasing groups are statistically  
121 indistinguishable (p-values of  $\sim 0.5$  and  $0.7$  for breached and unbreached populations respectively).  
122 We also map 7 strands, up to  $\sim 2$  km away from the rupturing fault. We mapped a total of 130 gaps,  
123 where only 5 were unbreached. The largest breached gap is  $\sim 15$  km long. Despite the low number  
124 of unbreached gaps mapped, the breached and unbreached ECDFs are statistically distinct (p-value  
125 of  $0.01$ ). Mapping an unbreached gap requires the rupturing fault and faults of parallel strike ahead  
126 of it to have been mapped in the regional map to a sufficient resolution to include gaps in the fault  
127 system. The low number of unbreached gaps we map may reflect the limited resolution of  
128 candidate, unactivated faults on available regional fault maps.

129 We map a total of 449 bends and analyze these separated into restraining versus releasing,  
130 and single versus double categories (Figure 2). The largest breached single bend is  $\sim 47^\circ$  and the  
131 largest breached double bend is  $\sim 42^\circ$ . The breached and unbreached single and double bends are  
132 statistically different ( $p = 3 \times 10^{-17}$  and  $p = 0.005$ ), but the breached restraining and releasing  
133 populations are not (p-values of  $0.1$  and  $0.7$  for breached and unbreached respectively).

134 We map 47 splays. The angles of splays that were ruptured versus splays that were  
135 bypassed cannot be separated by the KS test ( $p = 0.7$ ). In most cases where a splay was activated,

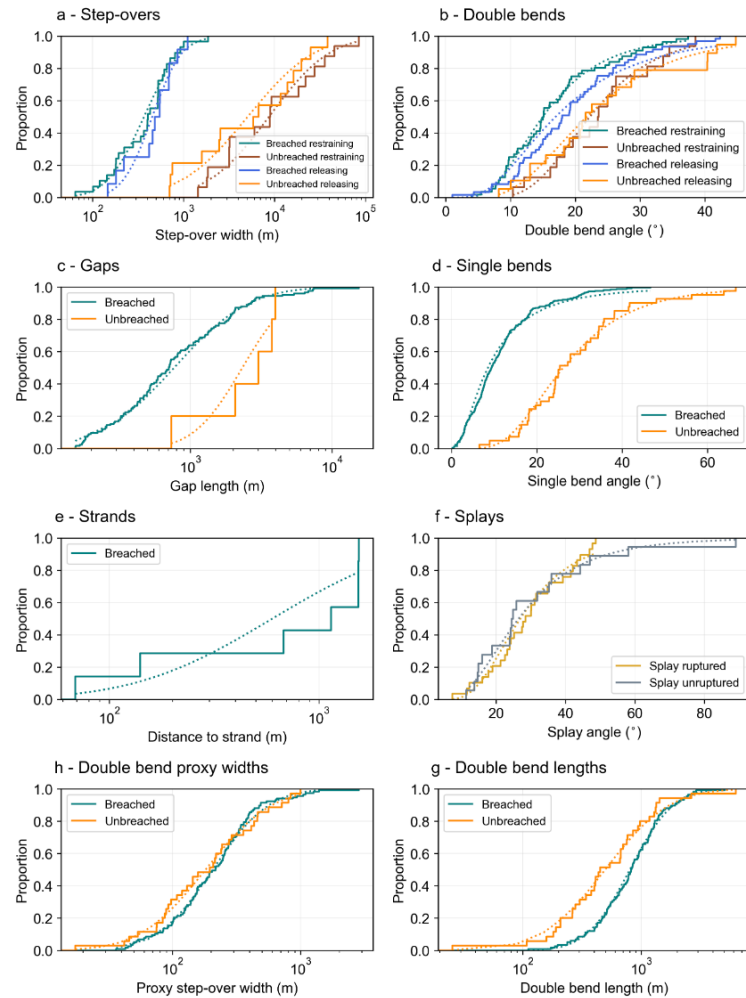
136 the rupture propagated less than 3 km onto the splay fault. Modeling studies suggest rupture arrest  
137 at splays is related to the kinematics of the junction and the length of the fault branch (Poliakov et  
138 al., 2002; Kame et al., 2004). Though we do not classify our splays into transpressional or  
139 transtensional because the direction of rupture propagation is only known for some events, the fact  
140 that we only observe two complete rupture arrests at splays suggests that the presence of a splay  
141 plays a small role in the behavior of the rupture on the principal fault, despite the fact that most  
142 splay branches mapped were relatively short, which should hinder rupture propagation by allowing  
143 the two fault segments to interact as the rupture stops on the shorter one (Bhat et al., 2007). Overall,  
144 our results suggest that splays do not play an important role in rupture arrest at the mapping scale  
145 and that small splays may be surficial features without depth-persistence.

146 An important difference between characterizing step-overs from simplified rupture maps  
147 and the detailed rupture maps in the FDHI database is that the simplified rupture maps may not  
148 include linking structures. Breached step-overs wider than 2 km measured in previous work (e.g.  
149 Lettis et al., 2002) are hard-linked by faults in the more detailed rupture maps. We classify these  
150 hard-linked steps as breached double bends or splays, depending on what feature achieves the  
151 linkage. This is the case for the steps along the Landers earthquake which are hard linked by splay  
152 faults and were previously described as “complex step-overs” (e.g., Biasi and Wesnousky, 2016).

153 As part of their evolution, step-overs can become hard-linked by fault segments, evolving  
154 into double bends (Figure S1). We analyze our bend population by looking at two additional  
155 geometrical characteristics, a bend length (Lozos et al., 2011), and a proxy step-over width (Figure  
156 S1). When we parameterize bends by length or proxy step-over width, we find no clear differences  
157 between the breached and unbreached populations (Figure 2h, g). This suggests that step-overs  
158 that evolve into double bends become mechanically different features with higher passing  
159 probability for the same (proxy) width. An important implication of this observation is that the  
160 hard linkage we observe at the surface may persist at depth. This supports that earthquake gates of  
161 small dimensions can span the entire seismogenic zone and play a role in modulating rupture  
162 dynamics.

163 Rupture termination sometimes occurs on a straight portion of a fault, absent an observed  
164 earthquake gate, where the active fault continues for at least one kilometer past the rupture tip.

165 This is the case for ~20% of the rupture termini in this study, comparable to the 10% of Biasi and  
 166 Wesnousky (2016), who used a five-kilometer threshold for rupture continuation.



167

168 **Figure 2.** Empirical cumulative distribution function for the features mapped in this study (solid)  
 169 and log-normal cumulative distribution fit for each ECDF (dotted). a: Restraining and releasing  
 170 step-overs, parameterized based on width. b: Restraining and releasing double bends,  
 171 parameterized based on angle. c: Gap length. d: Single bends, parametrized based on angle. e:  
 172 Strands, parametrized based on their distance to the principal fault. f: Splays, separated into  
 173 ruptured or unruptured and categorized by angle. g: Double bend proxy step-over width (Figures  
 174 1 and S1). h: Double bend length.

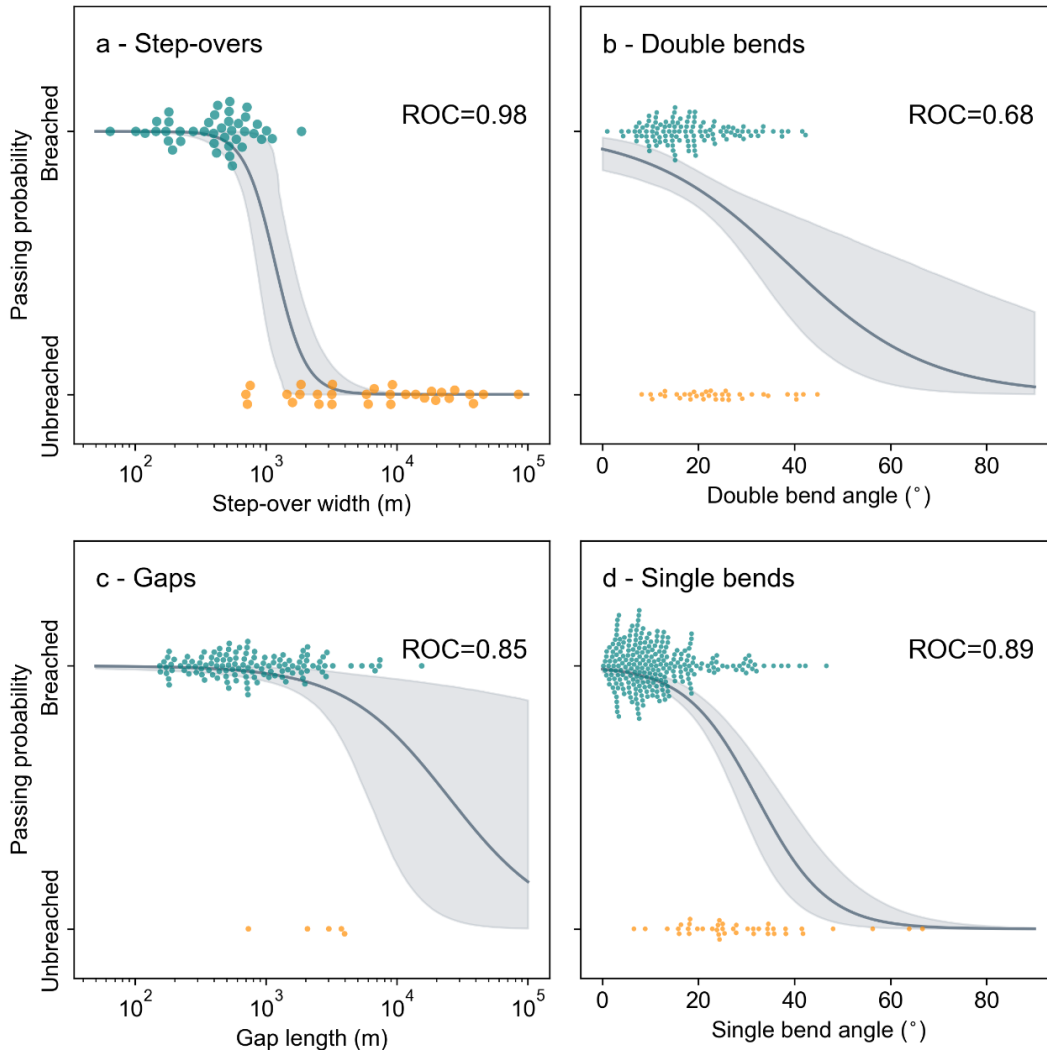
175

**176 Passing probabilities of earthquake gates**

177 Step-overs, gaps, and bends have statistically different breached and unbreached  
178 populations, acting as earthquake gates. We estimate passing probability as a function of geometry  
179 using a logistic model. This model describes the probability of a binary outcome (breached versus  
180 unbreached) as a continuous function of the geometrical properties of an earthquake gate, without  
181 requiring arbitrary binning of the data (see supplementary methods). We use unweighted logistic  
182 regressions despite the number of features in the breached and unbreached classes being different  
183 in the gaps and bends groups. We do this because, especially for the bends, the range of breached  
184 and unbreached bend angles largely overlaps, so that the relative frequency of breached and  
185 unbreached features is what distinguishes the two groups. Weighting the data inversely by  
186 frequency would obscure this effect.

187 Because restraining and releasing features are not statistically different, we combine these  
188 groups when estimating passing probabilities. Our logistic models (Figure 3) suggest that step-  
189 overs wider than  $\sim 1.2$  km will be breached less than half of the time. Step-overs  $>5$  km will be  
190 breached  $<1\%$  of the time, consistent with the fact that they are not observationally documented  
191 without linking structures in the rupture maps. The logistic models predict that gaps longer than  
192  $\sim 24.5$  km will be breached less than half of the time. This distance is considerably larger than for  
193 step-overs, which we interpret as evidence that the absence of sufficient unbreached gap  
194 measurements precludes a robust estimate of passing probabilities for gaps, or that gaps are not  
195 earthquake gates. Double bends  $>38^\circ$  and single bends  $>32^\circ$  are predicted to be breached less than  
196 half of the time.

197 We assess the performance of our logistic regressions using an ROC score and confusion  
198 matrix (Pedregosa et al., 2011, supplementary methods, Figures 3 and S3). Both metrics support  
199 that step-over width is a strong predictor of rupture arrest. The logistic regressions struggle to  
200 predict unbreached bends well. This is because the populations of breached and unbreached bends  
201 largely span the same bend angles and are only separated by the changes in the breached and  
202 unbreached frequency of that angle, which makes it difficult to predict with a binary classifier.  
203 Therefore, at the mapping scale, only large bend angles ( $>40^\circ$ ) consistently halt earthquake  
204 ruptures.



205

206 **Figure 3.** Logistic regressions (gray) showing the passing probabilities of geometrical features.  
 207 The data are shown as beehive plots, which show all data points in each classification, breached  
 208 in teal and unbreached in orange. Restraining and releasing features are combined (shown  
 209 separately in Figure S2). a: Passing probability as a function of step-over width. b: Passing  
 210 probability as a function of double bend angle. c: Passing probability versus gap length. d: Passing  
 211 probability as a function of single bend angle. The gray shading shows the 95% confidence interval  
 212 calculated by bootstrapping.

213 Biasi and Wesnousky (2016) predict step-overs wider than 3 km will be breached <50% of  
 214 the time. Three kilometers exceeds our largest observed breached step-over, which is ~1.8 km  
 215 wide. Biasi and Wesnousky (2017) also predict that bends sharper than 25° bend will be breached  
 216 <50%. These finding are consistent with the estimate of Ozawa et al. (2023) using quasi-dynamic

217 rupture models (Figure S4). We predict much larger passing probabilities of ~70% for single and  
 218 double bends of that size. The differences between our passing probabilities and those in previous  
 219 work arise from the use of different rupture maps (simplified versus not) and mapping at a finer  
 220 scale. Mechanically, breaching the larger bends we map may require a locally heterogeneous stress  
 221 field, as the large angle change would make the bend segment very incompatible with a uniform  
 222 stress field, even at low static friction values (Biasi and Wesnousky, 2017). A change in fault rake  
 223 from strike-slip to dip-slip could also explain larger bend angles but we lack the data to test this  
 224 option (see methods). Nevertheless, the fact that releasing and restraining features are statistically  
 225 indistinguishable (Figure 2) is also consistent with a locally heterogeneous stress field, since  
 226 homogeneous stress fields consistent yield distinctly different behavior for restraining and  
 227 releasing features (e.g. Lozos et al., 2011).

228 Whether surficial fault geometry corresponds to that at depth is a challenge for using  
 229 surface rupture maps to understand the physics of earthquake propagation. The different breached  
 230 and unbreached populations and associated passing probabilities we obtain suggest a correlation  
 231 between fault geometry at the surface and rupture propagation at depth. Together with the  
 232 difference in rupture behavior through step-overs and double bends of the same dimensions, this  
 233 suggests that the features we map at the surface, of 100-500 m length scales, extend downdip to  
 234 the seismogenic zone.

### 235 **Geometrical controls on surface rupture length**

236 For each of the events examined, we model an event likelihood that reflects the pre-existing  
 237 geometrical complexity in the hosting fault system as measured on the surface. We model event  
 238 likelihood as the joint likelihood of continuing past the collective straight fault segments,  $p(L)$ ,  
 239 and breaching  $n$  gates each with passing probability  $p_i$  in an event:  $P_{EQ} = P(L) \prod_{i=1}^N p_i$ . We  
 240 assume a constant chance of arrest at any point along without barriers and that the probabilities of  
 241 stopping at different barriers are independent. Accordingly, the probability that segments reach a  
 242 certain length in the absence of gates is the survival function of the exponential distribution,  
 243  $p(L) = e^{-\lambda L}$  where  $L$  is the rupture length, and  $\lambda = 1 \times 10^{-5}$  arrests/m is calculated by  
 244 dividing the total number of arrests on straight segments by the total rupture length of all events.  
 245 We derive passing probabilities for each feature as a function of its geometry from our logistic

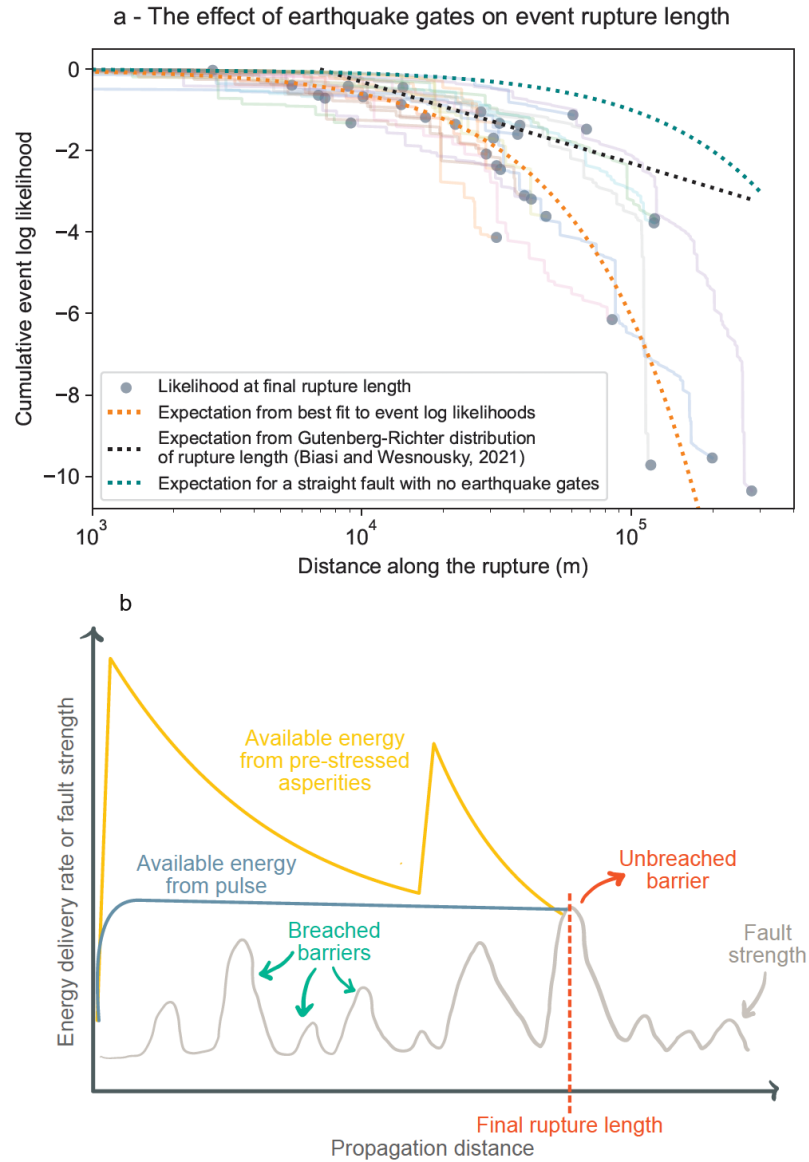
246 models (Figure 3). We exclude gaps from the likelihood estimates given the small number of  
247 unbreached gaps sampled and the fact that they do not clearly behave as gates.

248 To investigate the relationship of rupture length to event likelihood, we compute  
249 likelihoods as cumulative probabilities along each mapped rupture (Figure 4a), following a similar  
250 approach to Biasi and Wesnousky (2021). As ruptures encounter earthquake gates, the cumulative  
251 log-likelihood of each event decreases. Because these ruptures are long, gates with high passing  
252 probabilities contribute largely to reducing the event likelihood, even if their role in rupture arrest  
253 is unlikely. The final likelihood of each event is well related to the rupture length exponentially  
254 (Figure 4a), where the average spacing between neighboring gates is  $\sim 2$  km (Figure S5).

255 Earthquake scaling is typically considered in the context of the Gutenberg-Richter  
256 relationship, which predicts a power-law relationship between event frequency and rupture length  
257 (Figure 4a). Like in previous work on deriving probabilities from surface ruptures, the likelihood-  
258 length relationship does not match this prediction (Biasi and Wesnousky, 2021). With independent  
259 stopping probabilities at earthquake gates, as is inferred here, event likelihood will follow an  
260 exponential relationship, as opposed to a power law. To produce a power-law relationship would  
261 require that passing probabilities increase with rupture length, which is not supported by the  
262 observed distribution of earthquake gates (Figures 4a and S5). The Gutenberg-Richter relationship  
263 is defined for a population of earthquakes but may not fully describe the behavior of individual  
264 faults. Instead, each fault appears to have its own set of earthquake gates that contribute towards  
265 limiting rupture length. The possibility of non-Gutenberg-Richter behavior on a single fault is  
266 well-supported in the geological literature for surface-rupturing earthquakes (e.g. Schwartz and  
267 Coppersmith, 1984) but contrasts from the Gutenberg-Richter behavior associated with small  
268 earthquakes on single faults (Shelley et al., 2016). The distinction may have to do with the  
269 energetics of small versus seismogenic zone spanning events.

270 In this dataset, earthquakes often ended at barriers, where  $\sim 80\%$  of the rupture  
271 termini occurred at earthquake gates, supporting that barriers play a fundamental role in rupture  
272 arrest (Aki, 1979, 1989; King and Nabelek, 1985; Klinger et al., 2006; Rockwell and Klinger,  
273 2013). The distribution of breached barriers documented here also provide guidance on the  
274 appropriate model for rupture growth and propagation. An end-member model arising from linear  
275 elastic fracture mechanics is a crack with a uniform pre-stress in an infinite space, where the elastic

276 energy delivery rate would increase with rupture propagation length (e.g., Freund, 1998). In this  
277 model, stronger barriers would be required to stop rupture with greater propagation distance. We  
278 do not find a correlation between event size and barrier size, or barrier size along the rupture  
279 (Figures S6, S7 and S8). Therefore, this end-member is likely not appropriate and some  
280 heterogeneity in the stress field is required. An alternative crack-model with pre-stressed asperities  
281 results in a variable energy delivery rate (Lay and Kanamori, 1981; Li et al., 2023). Under this  
282 model, the available elastic energy is supplied by the asperities and decreases as the rupture  
283 propagates into regions with smaller pre-stress (Figure 4b). Seismological evidence supports that  
284 large surface rupturing events may be fueled by several asperities along the rupture (e.g. Li et al.,  
285 2023). This model predicts that larger gates would be breached in proximity to asperities, where  
286 the energy delivery rate is largest. We find no relationship between the geometry of breached gates  
287 and the distance to the event epicenter or the amplitude of the displacement, proxies for the  
288 locations of asperities (Figures S9 and S10), though the displacement data is limited for older  
289 events and certain regions. Pulses offer a third alternative. Ruptures tend to propagate as pulses  
290 once the seismogenic zone has been saturated (e.g. Heaton, 1990; Melgar and Hayes, 2017; Weng  
291 and Ampuero, 2019), which would result in a constant energy release rate under a homogeneous  
292 stress field. This model is consistent with the lack of correlation between breached gate size and  
293 location along the rupture, but incomplete, as some of our observations require a heterogeneous  
294 pre-stress distribution (e.g., large breached bend angles and indistinguishable releasing and  
295 restraining features). A propagating pulse encountering a collection of asperities of variable size  
296 that provide a variable energy delivery rate can explain both the observations requiring a  
297 heterogeneous pre-stress on the fault, and the absence of strong spatial relationships for the  
298 distribution of breached earthquake gates on the fault. Dynamic rupture models incorporating a  
299 distribution of earthquake gates similar to that described may provide a future test of this hybrid  
300 model.



301  
 302 **Figure 4.** a: Cumulative event likelihood versus distance along the surface rupture. Each colored  
 303 line represents one event. The scattered dots indicate the event likelihood at its final rupture length.  
 304 The rupture lengths are based on the FDHI event coordinate system (ECS) reference lines  
 305 (Sarmiento et al., 2021). The orange line represents the best fit to the final event likelihoods. The  
 306 black line represents the predicted decrease in event likelihood with rupture length using the  
 307 Gutenberg-Richter relationship for magnitude scaling. All likelihoods estimated using base  $e$ . b:  
 308 Schematic cartoon of how an earthquake gate will bring rupture to arrest, conditional on the  
 309 available elastic energy being lower than the strength of the barrier. Schematic elastic energy for  
 310 a crack with two pre-stressed asperities and a pulse in a homogeneous stress field shown.

311           When an earthquake terminates at a barrier, elevated residual stresses, if not relaxed, can  
312 promote rupture propagation past the barrier in a future event. This behavior is observed in multi-  
313 cycle rupture models (e.g., Duan and Oglesby, 2006; Molina-Ormazabal et al., 2023), laboratory  
314 experiments (Cebry et al., 2023), and inferred from the occurrence of aftershocks at barriers where  
315 ruptures terminate (Aki, 1979). Earthquake gates may therefore act as a barrier during an event,  
316 and as an asperity in a future one. The data in this study only permit assessing the behavior of  
317 individual gates over one earthquake cycle, but considering the data together offers insights into  
318 the frequency over which earthquake gates may act as an energy source, overlapping with locations  
319 of high slip on the fault, or energy sinks, overlapping with locations of low slip. We find that most  
320 of the large earthquake gates correspond with locations of low slip (Figure S10), consistent with  
321 ubiquitous barrier behavior, though small gates span a wide range of slip values. The very rare  
322 overlap of high slip values and unbreached earthquake gates suggests that, while earthquake gates  
323 may also act as asperities, this relationship is not frequent enough or the effect sufficiently large  
324 to stand out in our surface-rupture dataset. This is consistent with recent experimental work by  
325 Cebry et al. (2023), which showed that a high normal stress bump (a bend) behaved most  
326 frequently as a barrier but occasionally as an energy source, or asperity.

## 327 **Conclusions**

328           We map step-overs, bends, gaps, splays, and strands along the surface rupture maps of 31  
329 strike-slip earthquakes at 1:50,000 scale, labeling these features as breached and unbreached. We  
330 use these measurements to fit a logistic model to each feature that estimates passing probabilities  
331 as a function of geometry. Step-over width as measured at the surface is an excellent predictor of  
332 arrest. Bend angle is a worse predictor, although the ratio of unbreached to breached bends  
333 increases consistently with increasing bend angle. The fact that gates are preferred stopping points  
334 provides evidence that the surficial features can persist to depth. A more direct test of this idea is  
335 provided by the different behavior of step-overs and double bends of the same (proxy) width,  
336 which suggests that step-overs persist as discrete unlinked fault strands at depth. Our results call  
337 for models with geometrically complex faults consistent with our mapping scale to explore what  
338 dynamic rupture conditions may match our passing probabilities.

339           We use earthquake gate passing probabilities in each event to build an empirical model for

340 the growth and arrest of large earthquakes given the complexity of the hosting fault system. The  
341 cumulative event likelihood tabulated along rupture strike supports a barrier model as a factor in  
342 controlling earthquake size, where relatively straight fault segments are bounded by geometrical  
343 barriers that must be breached for the rupture to continue growing.

#### 344 **Acknowledgments**

345 We are grateful for comments from Julian Lozos and Glenn Biasi. We thank Coby Abrahams, Will  
346 Steindhart, Jean-Philippe Avouac, and Alexis Saez for suggestions and So Ozawa for sharing his  
347 data. S.W., V.H., and A.M.R.P. benefitted from mentoring from Gaby Noriega. A.M.R.P was  
348 supported by NASA FINESST award 80NSSC21K1634.

349

#### 350 **Open Research**

351 The rupture maps are available from the FDHI database (Sarmiento et al., 2021), accessed  
352 May 2022. Data and code can be accessed at [Data and code](#). All materials will be transferred to  
353 a Zenodo repository for permanent storage following acceptance.

#### 354 **References**

- 355 1. Aki, K. (1979). Characterization of barriers on an earthquake fault. *Journal of Geophysical*  
356 *Research: Solid Earth*, 84(B11), 6140-6148.
- 357 2. Aki, K. (1989). Geometric features of a fault zone related to the nucleation and termination  
358 of an earthquake rupture. In *Proceedings of Conference XLV. Fault Segmentation Controls*  
359 *of Rupture Initiation and Termination* (pp. 1-9).
- 360 3. Bachmanov, D.M., Trifonov, V.G., Kozhurin, A.I. and Zelenin E.A.: AFEAD v.2021  
361 *Active Faults of Eurasia Database*, <https://doi.org/10.13140/RG.2.2.10333.74726>, 2021.
- 362 4. Biasi, G. P., & Wesnousky, S. G. (2016). Steps and gaps in ground ruptures: Empirical  
363 bounds on rupture propagation. *Bulletin of the Seismological Society of America*, 106(3),  
364 1110-1124.
- 365 5. Biasi, G. P., & Wesnousky, S. G. (2017). Bends and ends of surface ruptures. *Bulletin of*  
366 *the Seismological Society of America*, 107(6), 2543-2560.
- 367 6. Biasi, G. P., & Wesnousky, S. G. (2021). Rupture passing probabilities at fault bends and  
368 steps, with application to rupture length probabilities for earthquake early warning. *Bulletin*

- 369 of the Seismological Society of America, 111(4), 2235-2247.
- 370 7. Cebry, S. B., Sorhaindo, K., & McLaskey, G. C. (2023). Laboratory earthquake rupture  
371 interactions with a high normal stress bump. *Journal of Geophysical Research: Solid*  
372 *Earth*, 128(11), e2023JB027297.
- 373 8. Crone, A. J., Personius, S. F., Craw, P. A., Haeussler, P. J., & Staff, L. A. (2004). The  
374 Susitna Glacier thrust fault: Characteristics of surface ruptures on the fault that initiated the  
375 2002 Denali fault earthquake. *Bulletin of the Seismological Society of America*, 94(6B),  
376 S5-S22.
- 377 9. Davy, P. (1993). On the frequency-length distribution of the San Andreas fault  
378 system. *Journal of Geophysical Research: Solid Earth*, 98(B7), 12141-12151.
- 379 10. Duan, B., & Oglesby, D. D. (2006). Heterogeneous fault stresses from previous  
380 earthquakes and the effect on dynamics of parallel strike-slip faults. *Journal of Geophysical*  
381 *Research: Solid Earth*, 111(B5).
- 382 11. Field, E. H., Biasi, G. P., Bird, P., Dawson, T. E., Felzer, K. R., Jackson, D. D., ... & Zeng,  
383 Y. (2015). Long-term time-dependent probabilities for the third Uniform California  
384 Earthquake Rupture Forecast (UCERF3). *Bulletin of the Seismological Society of America*,  
385 105(2A), 511-543.
- 386 12. Field, E. H., Jordan, T. H., Page, M. T., Milner, K. R., Shaw, B. E., Dawson, T. E., ... &  
387 Thatcher, W. R. (2017). A synoptic view of the third Uniform California Earthquake  
388 Rupture Forecast (UCERF3). *Seismological Research Letters*, 88(5), 1259-1267.
- 389 13. Hamling, I. J., Hreinsdóttir, S., Clark, K., Elliott, J., Liang, C., Fielding, E., ... & Stirling,  
390 M. (2017). Complex multifault rupture during the 2016 M w 7.8 Kaikōura earthquake, New  
391 Zealand. *Science*, 356(6334), eaam7194.
- 392 14. Heaton, T. H. (1990). Evidence for and implications of self-healing pulses of slip in  
393 earthquake rupture. *Physics of the Earth and Planetary Interiors*, 64(1), 1-20.
- 394
- 395 15. King, G., & Nábělek, J. (1985). Role of fault bends in the initiation and termination of  
396 earthquake rupture. *Science*, 228(4702), 984-987.
- 397 16. Klinger, Y., Michel, R., & King, G. C. (2006). Evidence for an earthquake barrier model  
398 from Mw~7.8 Kokoxili (Tibet) earthquake slip-distribution. *Earth and Planetary Science*  
399 *Letters*, 242(3-4), 354-364.

- 400 17. Klinger, Y. (2010). Relation between continental strike-slip earthquake segmentation and  
401 thickness of the crust. *Journal of Geophysical Research: Solid Earth*, 115(B7).
- 402 18. Langridge, R. M., Ries, W. F., Litchfield, N. J., Villamor, P., Van Dissen, R. J., Barrell, D.  
403 J. A., ... & Stirling, M. W. (2016). The New Zealand active faults database. *New Zealand*  
404 *Journal of Geology and Geophysics*, 59(1), 86-96.
- 405 19. Lay, T., & Kanamori, H. (1981). An asperity model of large earthquake  
406 sequences. *Earthquake prediction: An international review*, 4, 579-592.
- 407 20. Lettis, W., Bachhuber, J., Witter, R., Brankman, C., Randolph, C. E., Barka, A., ... & Kaya,  
408 A. (2002). Influence of releasing step-overs on surface fault rupture and fault segmentation:  
409 Examples from the 17 August 1999 Izmit earthquake on the North Anatolian fault,  
410 Turkey. *Bulletin of the Seismological Society of America*, 92(1), 19-42.
- 411 21. Lienkaemper, J. J., Pezzopane, S. K., Clark, M. M., & Rymer, M. J. (1987). Fault fractures  
412 formed in association with the 1986 Chalfant Valley, California, earthquake sequence:  
413 preliminary report. *Bulletin of the Seismological Society of America*, 77(1), 297-305.
- 414 22. Li, J., Kim, T., Lapusta, N., Biondi, E., & Zhan, Z. (2023). The break of earthquake  
415 asperities imaged by distributed acoustic sensing. *Nature*, 620(7975), 800-806.
- 416 23. Lozos, J. C., Oglesby, D. D., Duan, B., & Wesnousky, S. G. (2011). The effects of double  
417 fault bends on rupture propagation: A geometrical parameter study. *Bulletin of the*  
418 *Seismological Society of America*, 101(1), 385-398.
- 419 24. Manighetti, I., Campillo, M., Bouley, S., & Cotton, F. (2007). Earthquake scaling, fault  
420 segmentation, and structural maturity. *Earth and Planetary Science Letters*, 253(3-4), 429-  
421 438.
- 422 25. Melgar, D., & Hayes, G. P. (2017). Systematic observations of the slip pulse properties of  
423 large earthquake ruptures. *Geophysical Research Letters*, 44(19), 9691-9698.
- 424 26. Milner, K. R., Shaw, B. E., & Field, E. H. (2022). Enumerating plausible multifault  
425 ruptures in complex fault systems with physical constraints. *Bulletin of the Seismological*  
426 *Society of America*, 112(4), 1806-1824.
- 427 27. Molina-Ormazabal, D., Ampuero, J. P., & Tassara, A. (2023). Diverse slip behaviour of  
428 velocity-weakening fault barriers. *Nature Geoscience*, 16(12), 1200-1207.
- 429 28. Nurminen, F., Baize, S., Boncio, P., Blumetti, A. M., Cinti, F. R., Civico, R., & Guerrieri,  
430 L. (2022). SURE 2.0—New release of the worldwide database of surface ruptures for fault

- 431 displacement hazard analyses. *Scientific Data*, 9(1), 729.
- 432 29. Ozawa, S., Ando, R., & Dunham, E. M. (2023). Quantifying the probability of rupture  
433 arrest at restraining and releasing bends using earthquake sequence simulations. *Earth and*  
434 *Planetary Science Letters*, 617, 118276.
- 435 30. Pedregosa, F., Varoquaux, G., Gramfort, A., Michel, V., Thirion, B., Grisel, O., ... &  
436 Duchesnay, E. (2011). Scikit-learn: Machine learning in Python. *the Journal of machine*  
437 *Learning research*, 12, 2825-2830.
- 438 31. Perrin, C., Manighetti, I., Ampuero, J. P., Cappa, F., & Gaudemer, Y. (2016). Location of  
439 largest earthquake slip and fast rupture controlled by along-strike change in fault structural  
440 maturity due to fault growth. *Journal of Geophysical Research: Solid Earth*, 121(5), 3666-  
441 3685.
- 442 32. Rockwell, T. K., & Klinger, Y. (2013). Surface rupture and slip distribution of the 1940  
443 Imperial Valley earthquake, Imperial fault, southern California: Implications for rupture  
444 segmentation and dynamics. *Bulletin of the Seismological Society of America*, 103(2A),  
445 629-640.
- 446 33. Sarmiento, A., Madugo, D., Bozorgnia, Y., Shen, A., Mazzoni, S., Lavrentiadis, G.,  
447 Dawson, T., Madugo, C., Kottke, A., Thompson, S., Baize, S., Milliner, C., Nurminen, F.,  
448 Boncio, P., and Visini, F. (2021). Fault Displacement Hazard Initiative Database, UCL B.  
449 John Garrick Institute for the Risk Sciences, Report GIRS-2021-08, doi:  
450 10.34948/N36P48.
- 451 34. Schwartz, D. P., & Coppersmith, K. J. (1984). Fault behavior and characteristic  
452 earthquakes: Examples from the Wasatch and San Andreas fault zones. *Journal of*  
453 *Geophysical Research: Solid Earth*, 89(B7), 5681-5698.
- 454 35. Shelly, D. R., Ellsworth, W. L., & Hill, D. P. (2016). Fluid-faulting evolution in high  
455 definition: Connecting fault structure and frequency-magnitude variations during the 2014  
456 Long Valley Caldera, California, earthquake swarm. *Journal of Geophysical Research:*  
457 *Solid Earth*, 121(3), 1776-1795.
- 458 36. Styron, R., & Pagani, M. (2020). The GEM global active faults database. *Earthquake*  
459 *Spectra*, 36(1), 160-180.
- 460 37. U.S. Geological Survey, 2020, Quaternary Fault and Fold Database for the Nation,  
461 accessed [August, 10, 2022], at <https://doi.org/10.5066/P9BCVRCK>

- 462 38. Wells, D. L., & Coppersmith, K. J. (1993). Likelihood of surface rupture as a function of  
463 magnitude. *Seismological Research Letters*, 64(1), 54.
- 464 39. Wechsler, N., Ben-Zion, Y., & Christofferson, S. (2010). Evolving geometrical  
465 heterogeneities of fault trace data. *Geophysical Journal International*, 182(2), 551-567.
- 466 40. Weng, H., & Ampuero, J. P. (2019). The dynamics of elongated earthquake  
467 ruptures. *Journal of Geophysical Research: Solid Earth*, 124(8), 8584-8610.
- 468 41. Wesnousky, S. G. (1988). Seismological and structural evolution of strike-slip faults.  
469 *Nature*, 335(6188), 340-343.
- 470 42. Wesnousky, S. G. (2006). Predicting the endpoints of earthquake ruptures. *Nature*,  
471 444(7117), 358-360.
- 472 43. Wesnousky, S. G. (2008). Displacement and geometrical characteristics of earthquake  
473 surface ruptures: Issues and implications for seismic-hazard analysis and the process of  
474 earthquake rupture. *Bulletin of the Seismological Society of America*, 98(4), 1609-1632.